Title: Pharmacological, mechanistic and pharmacokinetic assessment of novel melatonin-tamoxifen drug conjugates as breast cancer drugs

Authors: Mahmud Hasan (1), Mohamed Akmal Marzouk (2), Saugat Adhikari (3), Thomas D. Wright (1), Benton P. Miller (1), Margarite D. Matossian (4,5), Steven Elliott (4,5), Maryl Wright (4,5), Madlin Alzoubi (4,5), Bridgette M. Collins-Burow (4,5), Matthew E. Burow (4,5), Ulrike Holzgrabe (6), Darius P. Zlotos (2), Robert E. Stratford (7) and Paula A. Witt-Enderby (1, 8)

Affiliations: 1. Duquesne University, Division of Pharmaceutical Sciences, Pittsburgh, PA 15282; 2. The German University in Cairo, Department of Pharmaceutical Chemistry, New Cairo City, 11835 Cairo, Egypt; 3. Purdue University, West Lafayette, IN; 4. Tulane University School of Medicine, Department of Medicine, Section of Hematology & Medical Oncology, New Orleans LA; 5. Tulane University School of Medicine, Tulane Cancer Center, New Orleans LA; 6. Institute of Pharmacy and Food Chemistry, University of Wuerzburg, Am Hubland, 97074 Wuerzburg, Germany; 7. Indiana University School of Medicine, Indianapolis, IN; 8. UPMC Hillman Cancer Center, Pittsburgh, PA 15232.

Journal title: Molecular Pharmacology

Legends:

Scheme 1. Synthesis of the melatonin-tamoxifen drug conjugates (C2, C4, C5, C9 and C15)

Figure 1. ^{1}H NMR (400 MHz, $CDCl_3$) and ^{13}C NMR (100 MHz, $CDCl_3$, including DEPT-135 subspectrum) spectra of the C2

Figure 2. ^{1}H NMR (400 MHz, $CDCl_3$) and ^{13}C NMR (100 MHz, $CDCl_3$, including DEPT-135 subspectrum) spectra of the C4

Figure 3. ^{1}H NMR (400 MHz, $CDCl_3$) and ^{13}C NMR (100 MHz, $CDCl_3$, including DEPT-135 subspectrum) spectra of the C5

Figure 4. ^{1}H NMR (400 MHz, $CDCl_3$) and ^{13}C NMR (100 MHz, $CDCl_3$, including DEPT-135 subspectrum) spectra of the C9

Figure 5. ^{1}H NMR (400 MHz, $CDCl_3$) and ^{13}C NMR (100 MHz, $CDCl_3$, including DEPT-135 subspectrum) spectra of the C15

Figure 6: Saturation of [^{3}H]-estradiol binding to ERs expressed in WT (A) and TamR (B) MCF-7 cells. Cell counting of WT and TamR MCF-7 cell lines treated with 100 nM of 4-OH-tamoxifen (C). Each bar represents total cell number (in ten thousand) expressed as mean ± SD. ** P<0.001 day 7 WT MCF-7 cell number vs. day 1 WT MCF-7 cell number by one-way ANOVA. *** P<0.001 day 3 and day 7 TamR MCF-7 cell number vs. day 1 TamR MCF-7 cell number by one-way ANOVA. ## P<0.01 day 3 TamR MCF-7 cell number vs. day 3 WT MCF-7 cell number by 2-way ANOVA with Bonferroni post hoc analysis. ### P<0.01 day 7 TamR MCF-7 cell number vs. day 7 WT MCF-7 cell number by two-way ANOVA with Bonferroni post hoc test. Immunocytochemistry images of MCF-7 (D) and TamR MCF-7 (E) cells. MCF-7 and TamR cells were treated with either vehicle or 100 nM 4-Hydroxytamoxifen for 24 hours. After treatment, cells were fixed in 4% Paraformaldehyde for 15 minutes. Cells were then permeabilized with 0.3% Triton-X followed by the addition of rabbit Ki67 and mouse ∝-Tubulin primary antibodies (1:1000, Cell Signaling). Goat anti-mouse Alexa Fluor 488 nm and goat anti-Rabbit Alexa Fluor 555 nm (1:1000, Invitrogen) were used as secondary antibodies. A Hoechst (Fisher) stain was used to visualize the nucleus. Images were obtained with the EVOS fluorescence inverted microscope (ThermoScientific, Waltham, MA) under 20x objective. Scale bar = 200 microns. Basal levels of pERK5, pERK1/2, ERα, NF-κB, and pAKT in TamR MCF-7 and MCF-7 cells (F). Bands were quantified using Image Studio™ Lite Software (LI-COR Biosciences, Lincoln, NE) and normalized against β-actin. Each bar represents the mean ± SD of 3 independent experiments. Data were analyzed by two-tailed t-test where a=p<0.05 vs TamR MCF-7. These TamR cells are consistent with literature demonstrating low ERα, high ERK5 and low ERK1/2 vs wildtype (Refs: Drew, B.A., Burow, M.E., Beckman, B.S. (2012) MEK5/ERK5 Pathway: The first fifteen years. *Biochim Biophys Acta*, 1825(1): 37–48; Mendes-Pereira, A. M., Sims, D., Dexter, T., Fenwick, K., Assiotis, I., Kozarewa, I., . . . Ashworth, A. (2012). Genome-wide functional screen identifies a compendium of genes affecting sensitivity to tamoxifen. *Proc Nat Acad Sci, 109*(8), 2730-2735; Vendrell, J. A., Robertson, K. E., Ravel, P., Bray, S. E., Bajard, A., Purdie, C. A., . . . Cohen, P. A. (2008). A candidate molecular signature associated with tamoxifen failure in primary breast cancer. *Breast Cancer Res, 10*(5), R88; Zhu, Y., Liu, Y., Zhang, C., Chu, J., Wu, Y., Li, Y., . . . Liu, Q. (2018). Tamoxifen-resistant breast cancer cells are resistant to DNA-damaging chemotherapy because of upregulated BARD1 and BRCA1. *Nature Communications, 9*(1), 1595.

Figure 7: Basal levels of pERK5, pERK1/2, NF-κB, RUNX2, β1-INTEGRIN and pAKT in MCF-7, MMC, MDA-MB-231, and BT-549 BC cells. Bands were quantified using Image Studio™ Lite (LI-COR Biosciences, Lincoln, NE) and normalized against β-actin. Each bar represents the mean ± SD of 3 independent experiments. Data were analyzed by one-way ANOVA followed by Newman-Keuls post-hoc t-test where a=p<0.05 vs MCF-7; b=p<0.05 vs MMC; c=p<0.05 vs MDA-MB-231.

Table 1: Mass Spectrometry Collision Parameters

Table 2: Mass Spectrometry Acquisition and Source Parameters

Table 3: Matrix Effect and Extraction Recovery

Table 4: The effect of MEK1/2 (PD98059) and MEK5 (Bix02189) on C4-mediated effects on pERK1/2, pERK5, NF-κB, RUNX2, β1-INTEGRIN levels in MCF-7, MMC, MDA-MB-231, and BT-549 cell lines. Bands were quantified using Image Studio™ Lite (LI-COR Biosciences, Lincoln, NE), where relative OD values were obtained. The data were then normalized against β-actin. Data represent the mean ± SD of three independent experiments. The lettering scheme is shown above each table where lower-case letters (e.g., a, b, c, etc.) indicate analysis done by one-way ANOVA followed by Newman-Keuls post hoc t-test. The upper-case letters (e.g., A, B, C) indicate two-tailed t-tests while the symbols (#, *, $) indicate one-tailed t-tests, where significance was defined as p<0.05.

Table 5: The effect of MEK1/2 (PD98059) and MEK5 (Bix02189) on C5-mediated effects on pERK1/2, pERK5, NF-κB, RUNX2 and β1-INTEGRIN levels in MCF-7, MMC, MDA-MB-231, and BT-549 cell lines. Bands were quantified using Image Studio™ Lite (LI-COR Biosciences, Lincoln, NE), where relative OD values were obtained. The data were then normalized against β-actin. Data represent the mean ± SD of three independent experiments. The lettering scheme is shown above each table where lower-case letters (e.g., a, b, c, etc.) indicate analysis done by one-way ANOVA followed by Newman-Keuls post hoc t-test. The upper-case letters (e.g., A, B, C) indicate two-tailed t-tests while the symbols (#, *, $) indicate one-tailed t-tests, where significance was defined as $p<0.05$.

Table 6: The effect of PI3K (pictilisib) on C4-mediated effects on pERK1/2, pERK5, NF-κB, RUNX2, β1-INTEGRIN and pAKT levels in MCF-7, MMC, MDA-MB-231, and BT-549 cell lines. Bands were quantified using Image Studio™ Lite (LI-COR Biosciences, Lincoln, NE), where relative OD values were obtained. The data were then normalized against β-actin. Data represent the mean ± SD of three independent experiments. The lettering scheme is shown above each table where lower-case letters (e.g., a, b, c, etc.) indicate analysis done by one-way ANOVA followed by Newman-Keuls post hoc t-test. The upper-case letters (e.g., A, B, C) indicate two-tailed t-tests while the symbols (#, *, $) indicate one-tailed t-tests, where significance was defined as $p<0.05$.

Table 7: The effect of PI3K (pictilisib) on C5-mediated effects on pERK1/2, pERK5, NF-κB, RUNX2, β1-INTEGRIN and pAKT levels in MCF-7, MMC, MDA-MB-231, and BT-549 cell lines. Bands were quantified using Image Studio™ Lite (LI-COR Biosciences, Lincoln, NE), where relative OD values were obtained. The data were then normalized against β-actin. Data represent the mean ± SD of three independent experiments. The lettering scheme is shown above each table where lower-case letters (e.g., a, b, c, etc.) indicate analysis done by one-way ANOVA followed by Newman-Keuls post hoc t-test. The upper-case letters (e.g., A, B, C) indicate two-tailed t-tests while the symbols (#, *, $) indicate one-tailed t-tests, where significance was defined as $p<0.05$.

Supplementary Material

Synthesis of the hybrid ligands

Our synthetic approach towards the melatonin-tamoxifen drug conjugates (C2, C4, C5, C9 and C15) is shown in Scheme 1. Briefly, *N*-desmethyltomoxifen (Gryder et al., 2013) was *N*-alkylated with $Br(CH_2)_nCO_2Me$ (n = 2,4,5,9,15). The products were subjected to ester hydrolysis and the resulting acids were coupled with *N*-desacetylmelatonin (Chatterjie at al., 2001) using EDCI HCl as a coupling reagent to give the final hybrid ligands. The identity and purity of the final compounds was confirmed by high-resolution ^{1}H and ^{13}C NMR spectra and by ESI mass spectra. The NMR spectra of all final compounds are shown in Figures 1-5. Full experimental details for the synthesis of C4 are given below.

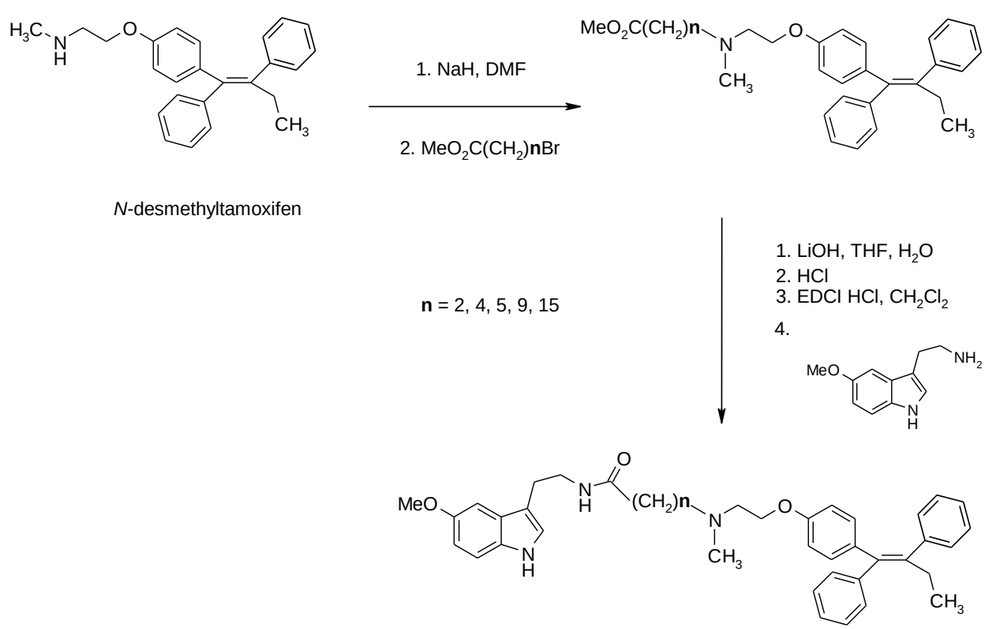

	n
C2	2
C4	4
C5	5
C9	9
C15	15

Scheme 1. Synthesis of the melatonin-tamoxifen drug conjugates (C2, C4, C5, C9 and C15)

General Methods. Column chromatography was carried out on silica gel 60 (0.063–0.200 mm) obtained from Merck. A Bruker AV-400 spectrometer was used to obtain ^{1}H NMR (400 MHz) and ^{13}C NMR (100 MHz) spectra respectively. Proton chemical shifts are referred to signals of $CHCl_3$ (7.26 ppm). Coupling constants (*J* values) are given in hertz (Hz). Carbon chemical shifts are referred to $CDCl_3$ (77.16 ppm). The NMR resonances were assigned by means of HH-COSY, and HMQC experiments. ESI mass spectra were determined on an Agilent 1100 MS systems. All reactions were carried out under an argon atmosphere. Column chromatography was carried out on silica gel 60 (0.063-0.200 mm) obtained from Merck (Darmstadt, Germany). All chemicals were purchased from commercial suppliers and used directly without any further purification.

Methyl 5-(*N*-desmethyltamoxifen-N-yl) pentanoate (1)

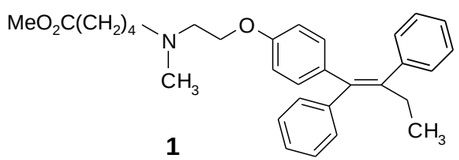

1

Sodium hydride (80 mg, 3.3 mmol) was added to a solution of *N*-desmethyltamoxifen (433 mg, 1.21 mmol) in dry DMF (20 mL) under ice-water cooling. After stirring for 15 min., methyl 5-bromovalerate (0.26 mL, 1.8 mmol) was added dropwise. After 30 min., the cooling bath was removed and stirring was continued for 24 h. Water (100 mL) was added and the mixture was extracted with ethyl acetate (3 x 20 mL). The organic layers were combined, washed with water, dried over sodium sulfate, and the solvent was evaporated under vacuum. The residue was subjected to column chromatography using ethyl acetate – methanol (10:2) to yield compound **1** (292 mg, 51 %) as a colorless oil. δ_H (400 MHz, $CDCl_3$) 0.93 (3H, t, *J* 7.4), 1.47- 1.55 (2H, m), 1.59 - 1.68 (2H, m), 2.31 (3H, s), 2.33 (2H, t, *J* 7.3), 2.45 – 2.50 (4H, m), 2.74 (2H, t, *J* 5.9), 3.65 (3H, s), 3.95 (2H, t, *J* 5.9), 6.52 – 6.58 (m, 2H), 6.74 – 6.81 (m, 2H), 7.10 – 7.14 (4H, m), 7.15 – 7.21 (2H, m), 7.23 – 7.29 (4H, m), 7.33 – 7.38 (2H, m). δ_c (100 MHz, $CDCl_3$) 13.7 (CH_3), 22.9 (CH_2), 26.6 (CH_2), 29.1 (CH_2), 34.0 (CH_2), 42.8 (CH_3), 51.6 (CH_3), 56.1 (CH_2), 57.7 (CH_2), 65.8 (CH_2), 113.5 (2 x CH), 126.1 (CH), 126.6 (CH), 128.0 (2 x CH), 128.2 (2 x CH), 129.6 (2 x CH), 129.8 (2 x CH), 132.0 (2 x CH), 135.7 (C) , 138.4 (C), 141.5 (C), 142.5 (C), 143.9 (C), 156.8 (C), 174.1(C).

5-[[4-[4-[(1*Z*)-1,2-diphenyl-1-buten-1-yl]phenoxy]ethyl]methylamino]-*N*-[2-(5-methoxy-1*H*-indol-3-yl)ethyl]pentanamide (**C4**).

2M aqueous LiOH solution (10 mL) was dropwise added to a solution of ester **1** (430 mg, 0.91 mmol) in THF (30 mL). After stirring for 24 h aqueous 1M HCl was dropwise added under ice-water cooling until the reaction mixture reached pH 6. The acid was extracted with dichloro-methane (3 x 20 mL), the organic layers were combined, dried over sodium sulfate, and the solvent was evaporated under vacuum to give the crude acid (301 mg) that was dissolved in dichloromethane (40 mL). EDCI HCl (151 mg, 0.79 mmol) was added under ice-water cooling and the mixture was stirred for 15 min followed by a dropwise addition of a solution of *N*-desacetylmelatonin (125 mg, 0.66 mmol) in dichloromethane (10 mL??). Cooling was removed, and the reaction mixture was stirred for 24 h. The solvent was removed under vacuum and the residue was subjected to column chromatography using dichloromethane – methanol (10:1) to yield the C4 (243 mg, 43%) as a colorless foam. δ_H (400 MHz, $CDCl_3$) 0.94 (3H, t, *J* 7.4), 1.41- 1.59 (2H, m), 1.53 - 1.64 (2H, m), 2.11 (2H, t, *J* 7.3), 2.25 (3H, s), 2.40 (2H, t, *J* 7.3),), 2.47 (2H, q, *J* 7.4), 2.69 (2H, t, *J* 5.7),), 2.91 (2H, t, *J* 6.6), 3.21 – 3.33 (1H, br), 3.56 (2H, q, *J* 6.6), 3.83 (3H, s), 3.90 (2H, t, *J* 5.7), 5.86 (1H, t, *J* 5.7), 6.51 – 6.55 (m, 2H), 6.77 – 6.80 (m, 2H), 6.84 (1H, dd, *J* 8.8, 2.4), 6.94 (1H, d, *J* 2.2), 7.02 (1H, d, *J* 2.4), 7.09 – 7.22 (6H, m), 7.23 – 7.30 (3H, m), 7.32 – 7.38 (2H, m), 8.53 (1H, s). δ_c (100 MHz, $CDCl_3$) 13.6 (CH_3), 23.5 (CH_2), 25.4 (CH_2), 26.3 (CH_2), 29.1 (CH_2), 36.4 (CH_2), 39.6 (CH_2), 42.5 (CH_3), 56.0 (CH_3), 56.1 (CH_2), 57.6 (CH_2), 65.4 (CH_2), 100.6 (CH), 112.16 (CH), 112.24 (CH), 112.5 (C), 113.4 (2 x CH), 123.1 (CH), 126.1 (CH), 126.6 (CH), 127.8 (C), 127.9 (2 x CH), 128.2 (2 x CH), 129.5 (2 x CH), 129.8 (2 x CH), 131.7 (C), 132.0 (2 x CH), 135.8 (C), 138.2 (C), 141.5 (C), 142.5 (C), 143.8 (C), 154.0 (C), 156.6 (C), 173.1(C). ESI MS *m/z* 630.5 $[M+1]^+$

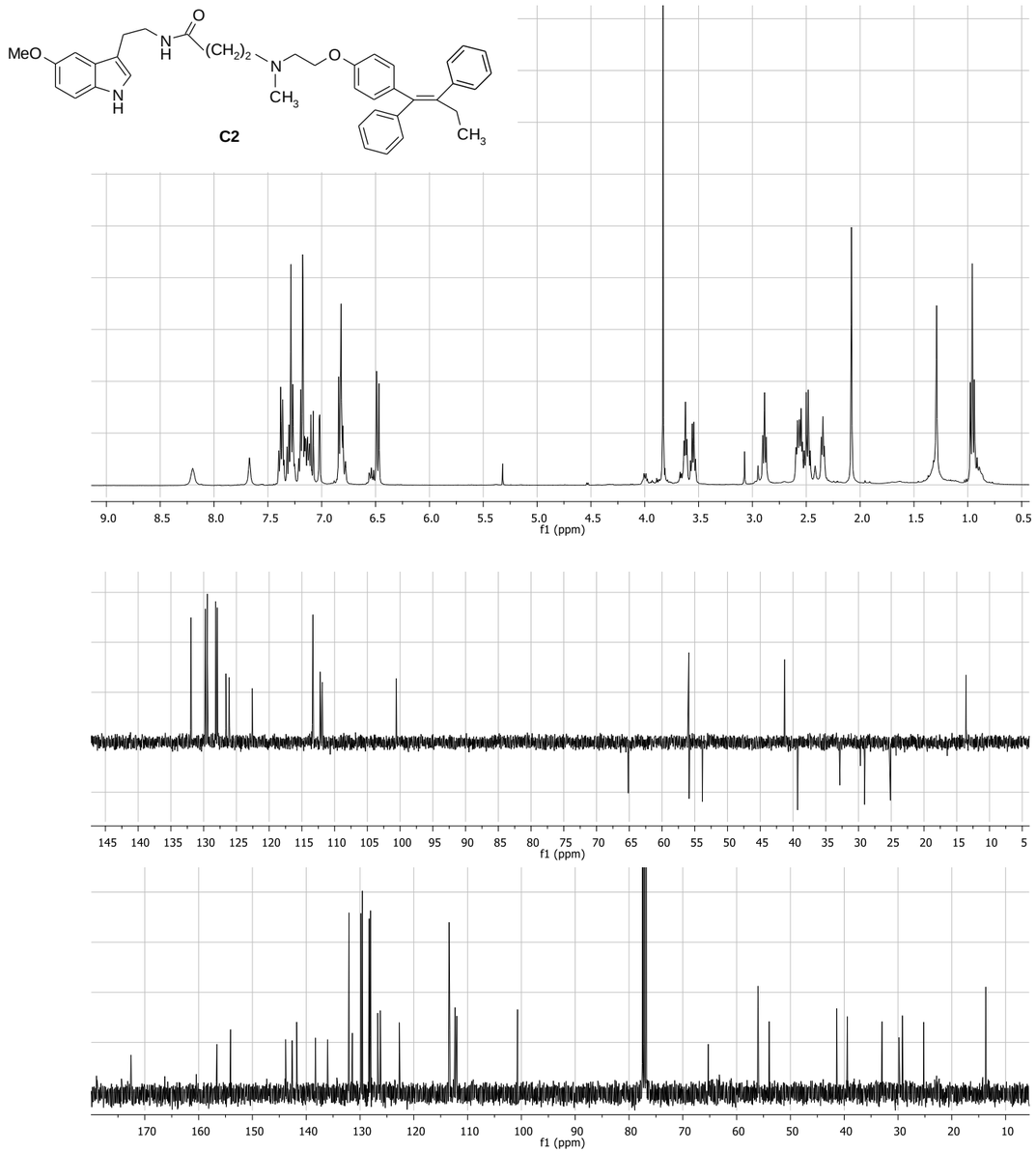

Figure 1. ^{1}H NMR (400 MHz, $CDCl_3$) and ^{13}C NMR (100 MHz, $CDCl_3$, including DEPT-135 subspectrum) spectra of the C2

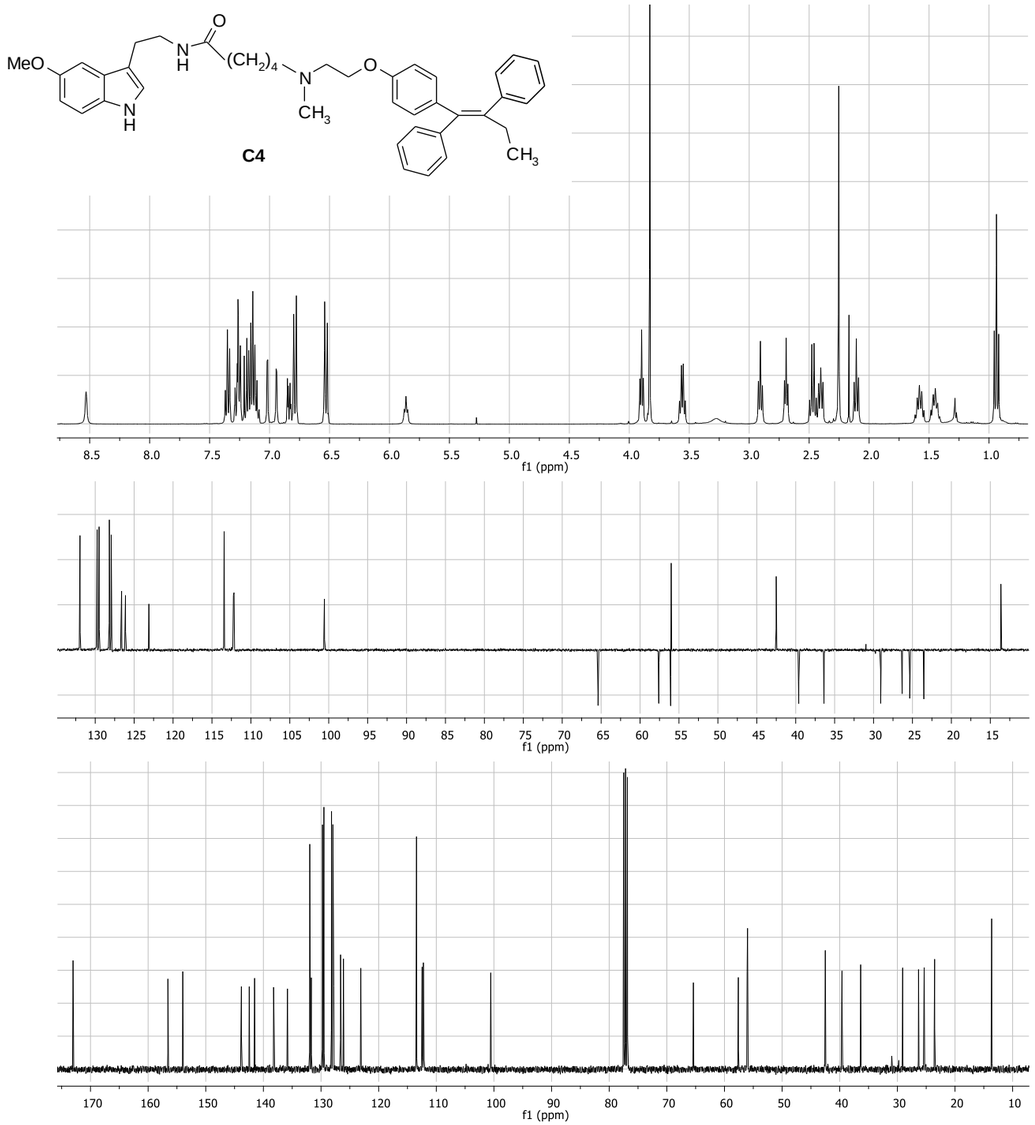

Figure 2. ^{1}H NMR (400 MHz, $CDCl_3$) and ^{13}C NMR (100 MHz, $CDCl_3$, including DEPT-135 subspectrum) spectra of the C4

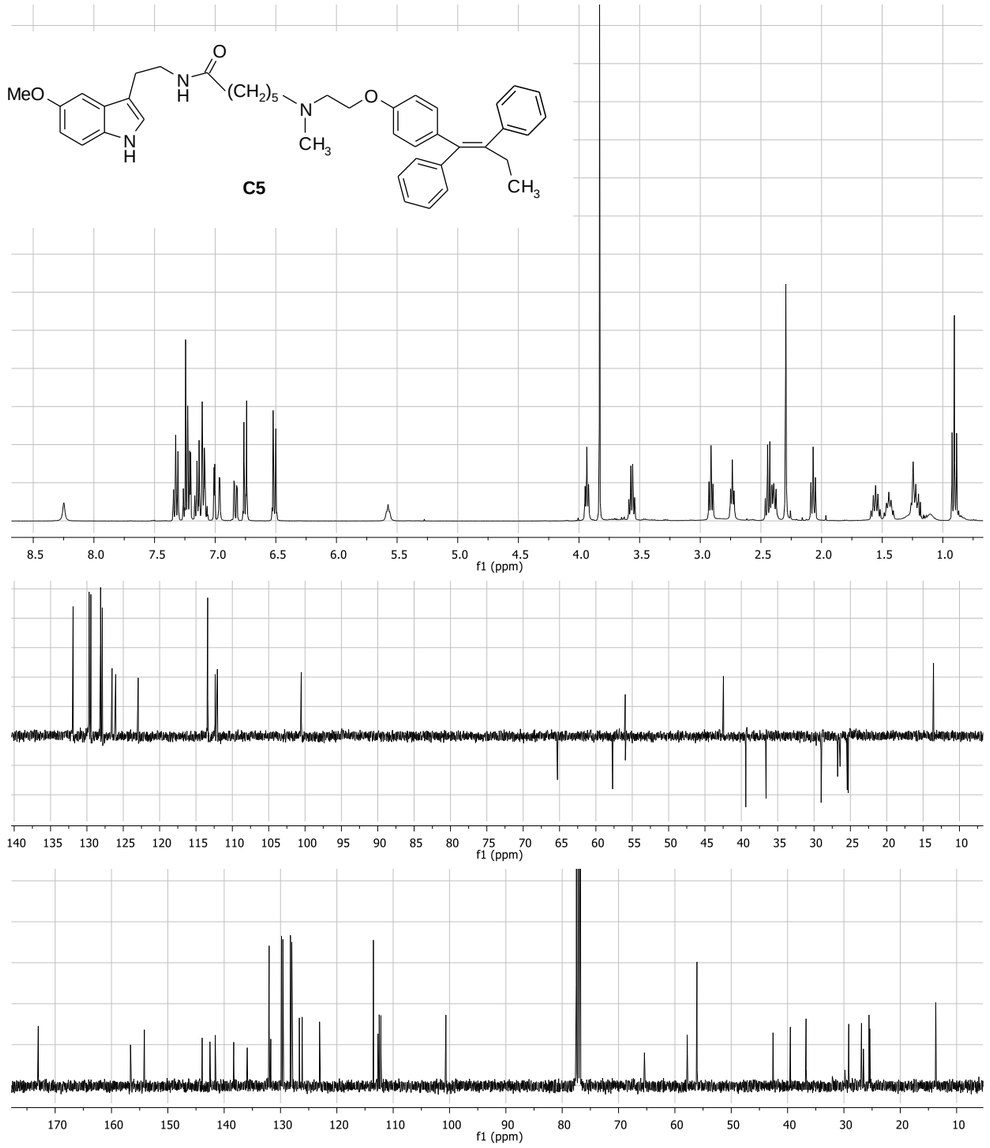

Figure 3. ^{1}H NMR (400 MHz, $CDCl_3$) and ^{13}C NMR (100 MHz, $CDCl_3$, including DEPT-135 subspectrum) spectra of the C5

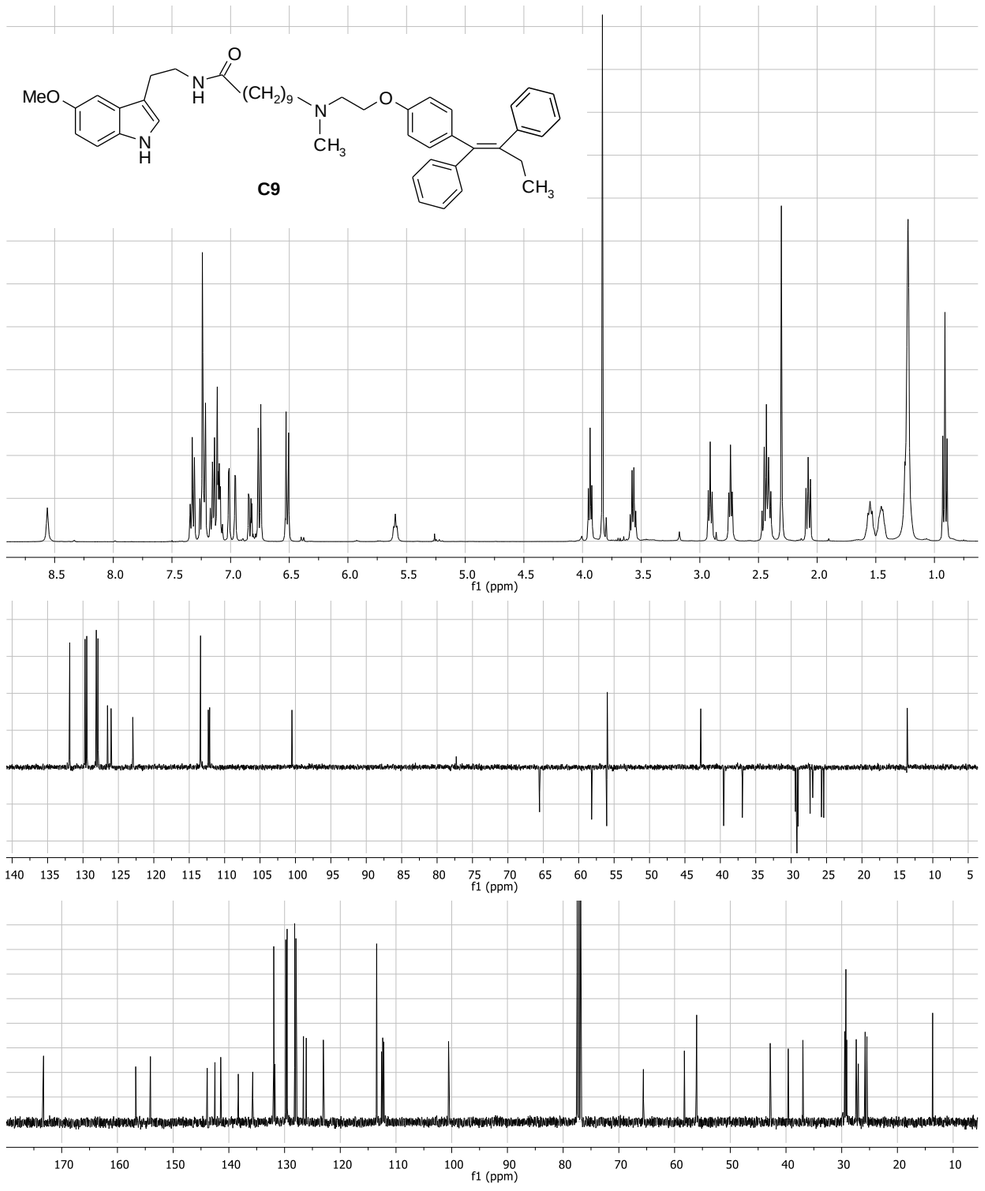

Figure 4. ^{1}H NMR (400 MHz, $CDCl_3$) and ^{13}C NMR (100 MHz, $CDCl_3$, including DEPT-135 subspectrum) spectra of the C9

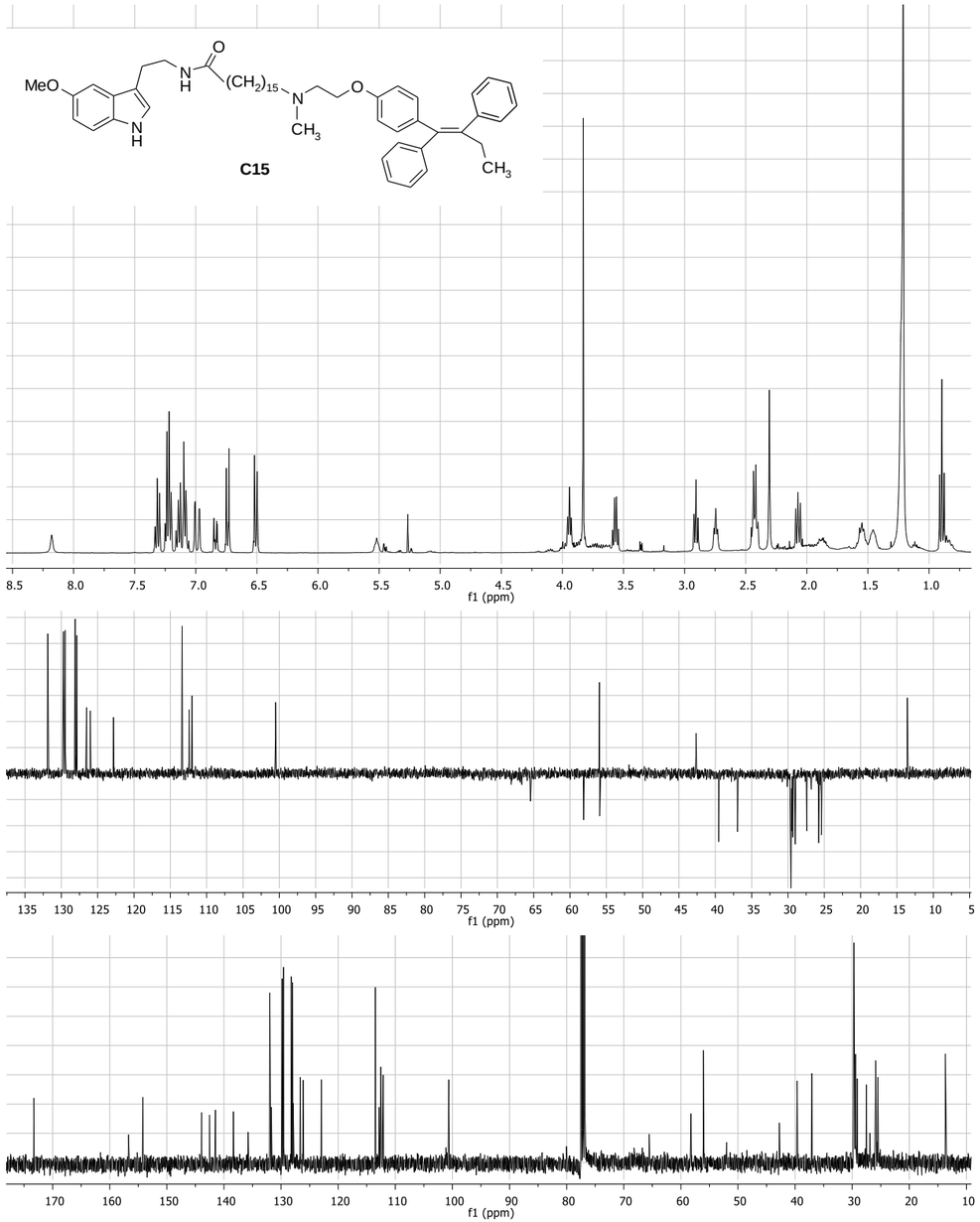

Figure 5. ^{1}H NMR (400 MHz, $CDCl_3$) and ^{13}C NMR (100 MHz, $CDCl_3$, including DEPT-135 subspectrum) spectra of the C15

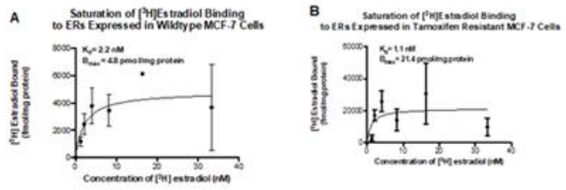
A
Saturation of [3H]Estradiol Binding
to ERs Expressed in Wildtype MCF-7 Cells
Concentration of [3H] estradiol (nM)

B
Saturation of [3H]Estradiol Binding
to ERs Expressed in Tamoxifen Resistant MCF-7 Cells
Concentration of [3H] estradiol (nM)

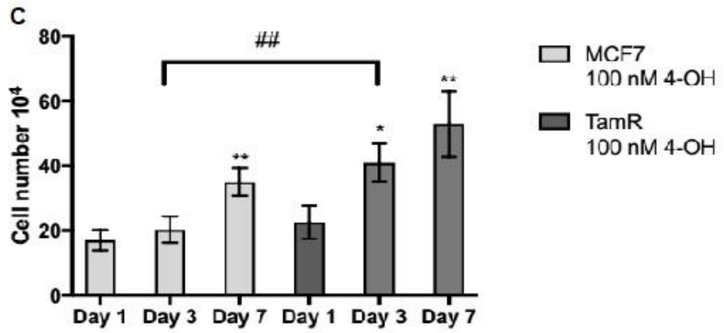
C
Cell number 10^4
##
*
**
**
Day 1
Day 3
Day 7
Day 1
Day 3
Day 7
MCF7
100 nM 4-OH
TamR
100 nM 4-OH

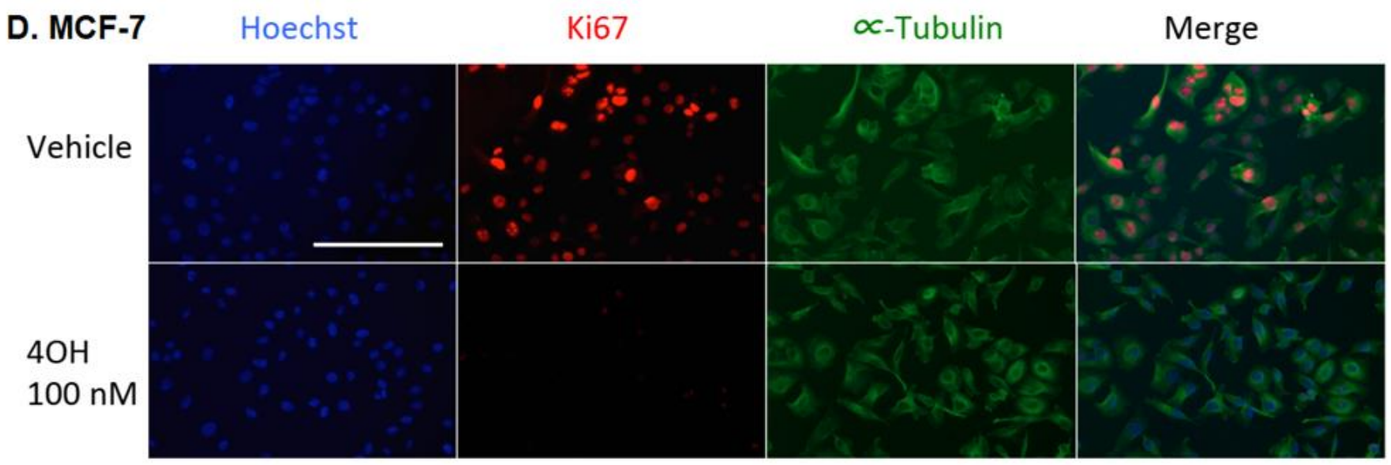
D. MCF-7
Hoechst
Ki67
∝-Tubulin
Merge
Vehicle
4OH
100 nM

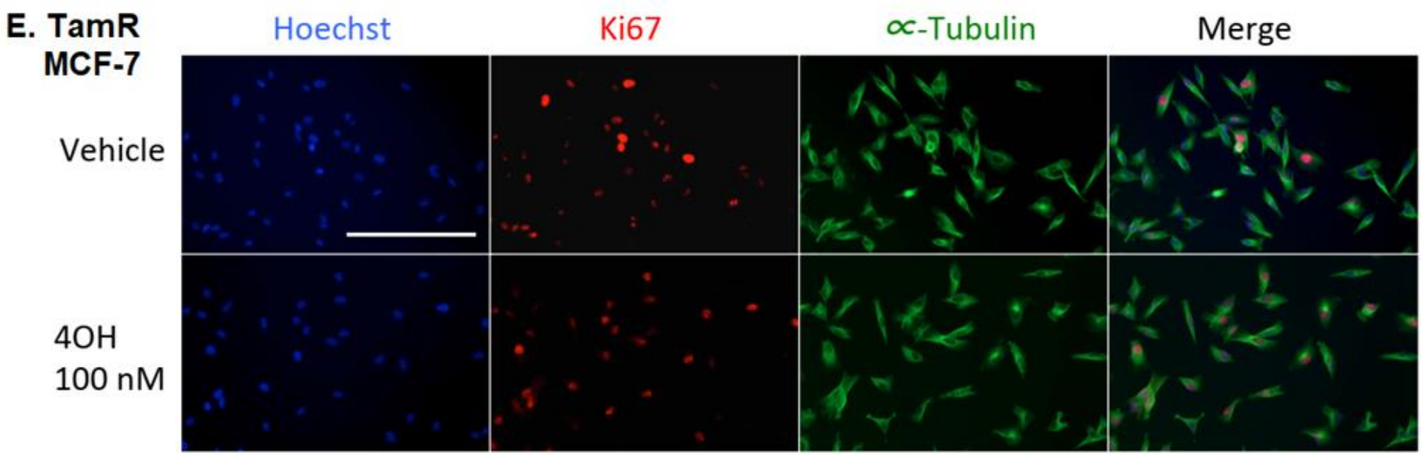
E. TamR
MCF-7
Hoechst
Ki67
∝-Tubulin
Merge
Vehicle
4OH
100 nM

F

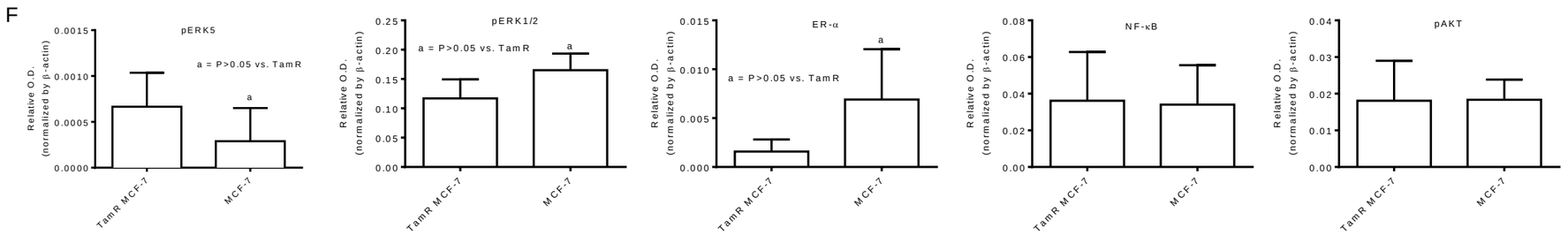

Figure 6: Saturation of [^{3}H]-estradiol binding to ERs expressed in WT (A) and TamR (B) MCF-7 cells. Cell counting of WT and TamR MCF-7 cell lines treated with 100 nM of 4-OH-tamoxifen (C). Each bar represents total cell number (in ten thousand) expressed as mean ± SD. ** P<0.001 day 7 WT MCF-7 cell number vs. day 1 WT MCF-7 cell number by one-way ANOVA. *** P<0.001 day 3 and day 7 TamR MCF-7 cell number vs. day 1 TamR MCF-7 cell number by one-way ANOVA. ## P<0.01 day 3 TamR MCF-7 cell number vs. day 3 WT MCF-7 cell number by 2-way ANOVA with Bonferroni post hoc analysis. ### P<0.01 day 7 TamR MCF-7 cell number vs. day 7 WT MCF-7 cell number by two-way ANOVA with Bonferroni post hoc test. Immunocytochemistry images of MCF-7 (D) and TamR MCF-7 (E) cells. MCF-7 and TamR cells were treated with either vehicle or 100 nM 4-Hydroxytamoxifen for 24 hours. After treatment, cells were fixed in 4% Paraformaldehyde for 15 minutes. Cells were then permeabilized with 0.3% Triton-X followed by the addition of rabbit Ki67 and mouse ∝-Tubulin primary antibodies (1:1000, Cell Signaling). Goat anti-mouse Alexa Fluor 488 nm and goat anti-Rabbit Alexa Fluor 555 nm (1:1000, Invitrogen) were used as secondary antibodies. A Hoechst (Fisher) stain was used to visualize the nucleus. Images were obtained with the EVOS fluorescence inverted microscope (ThermoScientific, Waltham, MA) under 20x objective. Scale bar = 200 microns. Basal levels of pERK5, pERK1/2, ERα, NF-κB, and pAKT in TamR MCF-7 and MCF-7 cells (F). Bands were quantified using Image Studio™ Lite Software (LI-COR Biosciences, Lincoln, NE) and normalized against β-actin. Each bar represents the mean ± SD of 3 independent experiments. Data were analyzed by two-tailed t-test where a=p<0.05 vs TamR MCF-7. These TamR cells are consistent with literature demonstrating low ERα, high ERK5 and low ERK1/2 vs wildtype (Refs: Drew, B.A., Burow, M.E., Beckman, B.S. (2012) MEK5/ERK5 Pathway: The first fifteen years. *Biochim Biophys Acta*, 1825(1): 37–48; Mendes-Pereira, A. M., Sims, D., Dexter, T., Fenwick, K., Assiotis, I., Kozarewa, I., . . . Ashworth, A. (2012). Genome-wide functional screen identifies a compendium of genes affecting sensitivity to tamoxifen. *Proc Nat Acad Sci, 109*(8), 2730-2735; Vendrell, J. A., Robertson, K. E., Ravel, P., Bray, S. E., Bajard, A., Purdie, C. A., . . . Cohen, P. A. (2008). A candidate molecular signature associated with tamoxifen failure in primary breast cancer. *Breast Cancer Res, 10*(5), R88; Zhu, Y., Liu, Y., Zhang, C., Chu, J., Wu, Y., Li, Y., . . . Liu, Q. (2018). Tamoxifen-resistant breast cancer cells are resistant to DNA-damaging chemotherapy because of upregulated BARD1 and BRCA1. *Nature Communications, 9*(1), 1595.

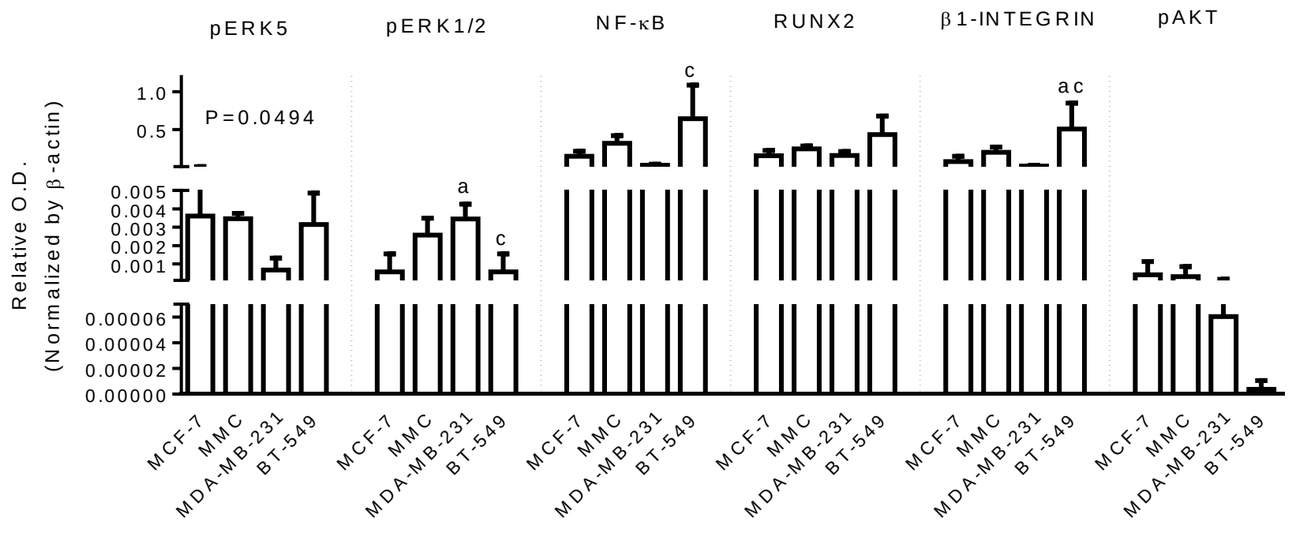

Figure 7: Basal levels of pERK5, pERK1/2, NF-κB, RUNX2, β1-INTEGRIN and pAKT in MCF-7, MMC, MDA-MB-231, and BT-549 BC cells. Bands were quantified using Image Studio™ Lite (LI-COR Biosciences, Lincoln, NE) and normalized against β-actin. Each bar represents the mean ± SD of 3 independent experiments. Data were analyzed by one-way ANOVA followed by Newman-Keuls post-hoc t-test where a=p<0.05 vs MCF-7; b=p<0.05 vs MMC; c=p<0.05 vs MDA-MB-231.

Table 1: Mass Spectrometry Collision Parameters

Compounds	**Parent (m/z)**	**Daughter (m/z)**	**Collision Energy (V)**
Tamoxifen (TAM)	372.2	72.1	21
TAM-d5	377.2	72.1	21
C4	630.4	174.1	45
C5	644.4	174.1	45

Table 2: Mass Spectrometry Acquisition and Source Parameters

Source parameters	**Conditions**	**Acquisition parameters**	**Conditions**
Gas Temperature	320 °C	Dwell time	200 ms
Gas Flow	10 l/min	Fragmentor Voltage	135 V
Nebulizer	45 psi	Cell Accelerator Voltage	7 V
Sheath gas Temp	370 °C	Polarity	positive
Sheath gas Flow	11 l/min		
Capillary Voltage	3500 V		
Nozzle Voltage	500		

Table 3: Matrix Effect and Extraction Recovery

Compounds	**Matrix effect (%) Mean ± SD**	**Extraction Recovery (%) Mean± SD**
Tamoxifen	10.75 ± 7.76 [a]	94.34 ± 14.41 [a]
C4	8.47 ± 8.64 [a]	96.9 ± 29.92 [a]
C5	11.32 ± 6.85 [b]	105.27 ± 6.18 [c]

[a] n = 7, [b] n = 6, [c] n = 4

Table 4: The effect of MEK1/2 (PD98059) and MEK5 (Bix02189) on C4-mediated effects on pERK1/2, pERK5, NF-κB, RUNX2, β1-INTEGRIN levels in MCF-7, MMC, MDA-MB-231, and BT-549 cell lines. Bands were quantified using Image Studio™ Lite (LI-COR Biosciences, Lincoln, NE), where relative OD values were obtained. The data were then normalized against β-actin. Data represent the mean ± SD of three independent experiments. The lettering scheme is shown above each table where lower-case letters (e.g., a, b, c, etc.) indicate analysis done by one-way ANOVA followed by Newman-Keuls post hoc t-test. The upper-case letters (e.g., A, B, C) indicate two-tailed t-tests while the symbols (#, *, $) indicate one-tailed t-tests, where significance was defined as $p<0.05$.

	MCF-7	Veh (*A)	1 nM C4(#B)	1 nM C5 ($C)	10 µM Bix02189	1 nM C4+10 µM Bix02189	1nM C5+10 µM Bix02189	10 µM PD98059	1 nM C4+10 µM PD98059	1 nM C5+10 µM PD98059
pERK1/2		0.00092±0.001	0.018±0.024	0.0093±0.003 (*A)	0.004±0.002 (*A)	0.0018±0.001	0.0022±0.001 ($C)	0.00039±0.0005 (*A)	0.0012±0.001	0.0021±0.001 ($C)
pERK5		0.02±0.022	0.31±0.421	0.051±0.027	0.044±0.038	0.038±0.0012	0.055±0.022	0.035±0.028	0.016±0.022	0.031±0.005
NF-κB		0.045±0.030	0.085±0.056	0.14±0.074 (*A)	0.091±0.053	0.09±0.032	0.099±0.052	0.085±0.023	0.067±0.022	0.078±0.033
RUNX2		0.0048±0.005	0.043±0.069	0.010±0.011	0.0088±0.009	0.0078±0.009	0.0081±0.009	0.0066±0.004	0.0067±0.007	0.0077±0.011
	MMC	Veh (*A)	1 nM C4(#B)	1 nM C5 ($C)	10 µM BIX	1 nM C4+BIX	1 nM C5+BIX	10 µM PD	1 nM C4+PD	1 nM C5+PD
pERK1/2		0.0092±0.004	0.0054±0.001	0.005±0.001	0.0076±0.005	0.015±0.007	0.018±0.007 ($C)	0.0082±0.003	0.014±0.001 (#B)	0.013±0.006
pERK5		0.041±0.027	0.05±0.018	0.079±0.053	0.071±0.059	0.093±0.008 (#)	0.078±0.015	0.06±0.035 (*)	0.07±0.008	0.058±0.034
NF-κB		0.12±0.051	0.1±0.010	0.12±0.038	0.13±0.067	0.2±0.220	0.1±0.078	0.12±0.036	0.14±0.016 (#B)	0.16±0.041
RUNX2		0.00041±0.0002	0.00049±0.0005	0.00079±0.0003	0.00081±0.0001	0.0014±0.001	0.00084±0.0004	0.00074±0.0003	0.00073±0.0002	0.0008±0.0005
	MDA-MB-231	Veh (*A)	1 nM C4(#B)	1 nM C5 ($C)	10 µM BIX	1 nM C4+BIX	1 nM C5+BIX	10 µM PD	1 nM C4+PD	1 nM C5+PD
pERK1/2		0.038±0.017	0.051±0.018	0.063±0.021	0.039±0.015	0.038±0.005	0.049±0.011	0.027±0.012	0.014±0.005 (#B)	0.012±0.009 ($C)
pERK5		0.0028±0.006	0.0029±0.002	0.0091±0.005	0.0087±0.008	0.0042±0.007	0.0044±0.006	0.011±0.007 (*)	0.0085±0.010	0.0018±0.003
NF-κB		0.022±0.021	0.032±0.018	0.043±0.012	0.062±0.047 (*)	0.035±0.003	0.06±0.005	0.085±0.019	0.093±0.037 (#)	0.13±0.046
RUNX2		0.00049±0.0003	0.00073±0.0003	0.00062±0.0002	0.00065±0.0004	0.00048±0.0004	0.0013±0.001	0.00072±0.0005	0.00046±0.0001	0.00098±0.0008
	BT-549	Veh (*A)	1 nM C4(#B)	1 nM C5 ($C)	10 µM BIX	1 nM C4+BIX	1 nM C5+BIX	10 µM PD	1 nM C4+PD	1 nM C5+PD
pERK1/2		0.00033±0.0006	0±0	0±0	0.000063±0.0001	0±0	0±0	0±0	0±0	0±0
pERK5		0.018±0.014	0.029±0.012	0.033±0.0012	0.042±0.021	0.033±0.006	0.023±0.007	0.0094±0.009	0.013±0.015	0.011±0.018
NF-κB		0.058±0.019	0.07±0.011	0.076±0.013	0.079±0.013	0.091±0.016	0.065±0.005	0.047±0.019	0.054±0.023	0.03±0.028
RUNX2		0.013±0.011	0.013±0.0008	0.016±0.002	0.016±0.007	0.018±0.006	0.014±0.001	0.016±0.005	0.014±0.007	0.017±0.007

Table 5: The effect of MEK1/2 (PD98059) and MEK5 (Bix02189) on C5-mediated effects on pERK1/2, pERK5, NF-κB, RUNX2 and β1-INTEGRIN levels in MCF-7, MMC, MDA-MB-231, and BT-549 cell lines. Bands were quantified using Image Studio™ Lite (LI-COR Biosciences, Lincoln, NE), where relative OD values were obtained. The data were then normalized against β-actin. Data represent the mean ± SD of three independent experiments. The lettering scheme is shown above each table where lower-case letters (e.g., a, b, c, etc.) indicate analysis done by one-way ANOVA followed by Newman-Keuls post hoc t-test. The upper-case letters (e.g., A, B, C) indicate two-tailed t-tests while the symbols (#, *, $) indicate one-tailed t-tests, where significance was defined as $p<0.05$.

	MCF-7	Veh (*A)	10 μM C4 (#B)	10 μM C5 ($C)	10 μM Bix02189	10 μM C4+10 μM Bix02189	10 μM C5+10 μM Bix02189	10 μM PD98059	10 μM C4+10 μM PD98059	10 μM C5+10 μM PD98059
pERK1/2		0.00092±0.0006	0.0042±0.004 (*A)	0.0047±0.003 (*)	0.004±0.002 (*A)	0.0039±0.001	0.0028±0.001	0.00039±0.0005	0±0	0±0 ($)
pERK5		0.02±0.022	0.072±0.064	0.032±0.043	0.044±0.038	0.043±0.032	0.035±0.038	0.035±0.028	0.032±0.028	0.023±0.020
NF-κB		0.045±0.030	0.16±0.085 (*A)	0.13±0.068 (*A)	0.091±0.053	0.12±0.028	0.11±0.011	0.085±0.023 (*A)	0.096±0.019	0.072±0.005
RUNX2		0.0048±0.005	0.012±0.009	0.01±0.007	0.0088±0.009	0.0085±0.007	0.0072±0.007	0.0066±0.004	0.0064±0.004	0.0052±0.007
	MMC	Veh (*A)	10 μM C4 (#B)	10 μM C5 ($C)	10 μM BIX	10 μM C4+BIX	10 μM C5+BIX	10 μM PD	10 μM C4+PD	10 μM C5+PD
pERK1/2		0.0092±0.004	0.0084±0.007	0.0053±0.004	0.0076±0.005	0.0045±0.002	0.0052±0.002	0.0082±0.003	0.014±0.004	0.0061±0.002
pERK5		0.041±0.027	0.067±0.064	0.023±0.031	0.071±0.059	0.043±0.022	0.075±0.063	0.06±0.035	0.043±0.042	0.067±0.009
NF-κB		0.12±0.051	0.15±0.115	0.16±0.145	0.13±0.067	0.071±0.076	0.097±0.026	0.12±0.036	0.14±0.026	0.13±0.026
RUNX2		0.00041±0.0002	0.00075±0.0002	0.00073±0.0003	0.00081±0.0001	0.00063±0.0005	0.00069±0.0006	0.00074±0.0003	0.001±0.0003	0.00079±0.0002
	MDA-MB-231	Veh (*A)	10 μM C4 (#B)	10 μM C5 ($C)	10 μM BIX	10 μM C4+BIX	10 μM C5+BIX	10 μM PD	10 μM C4+PD	10 μM C5+PD
pERK1/2		0.038±0.017	0.026±0.026	0.033±0.006	0.039±0.015	0.032±0.017	0.037±0.011	0.027±0.012	0.032±0.011	0.014±0.003 ($C)
pERK5		0.0028±0.006	0.004±0.003	0.0071±0.004	0.0087±0.008	0.0091±0.003	0.013±0.010	0.011±0.007	0.018±0.001 (#B)	0.014±0.004
NF-κB		0.022±0.021	0.043±0.055 (*)	0.054±0.017	0.062±0.047	0.083±0.008	0.072±0.038	0.085±0.019 (*A)	0.096±0.023	0.11±0.033
RUNX2		0.00049±0.0003	0.00049±0.0004	0.00047±0.0003	0.00065±0.0004	0.00095±0.0001	0.00074±0.0001	0.00072±0.0005	0.00059±0.0002	0.00048±0.0003
	BT-549	Veh (*A)	10 μM C4 (#B)	10 μM C5 ($C)	10 μM BIX	10 μM C4+BIX	10 μM C5+BIX	10 μM PD	10 μM C4+PD	10 μM C5+PD
pERK1/2		0.00033±0.0006	0±0	0±0	0.000063±0.0001	0±0	0±0	0±0	0±0	0±0
pERK5		0.018±0.014	0.021±0.011	0.026±0.022	0.042±0.021	0.026±0.002	0.0097±0.003	0.0094±0.009	0.00023±0.0003	0.00075±0.001
NF-κB		0.058±0.019	0.091±0.037	0.08±0.039	0.079±0.013	0.08±0.015	0.065±0.016	0.047±0.019	0.018±0.006 ($C)	0.0021±0.002
RUNX2		0.013±0.011	0.019±0.003	0.02±0.003	0.016±0.007	0.029±0.008	0.03±0.015	0.016±0.005	0.019±0.007	0.014±0.010

Table 6: The effect of PI3K (pictilisib) on C4-mediated effects on pERK1/2, pERK5, NF-κB, RUNX2, β1-INTEGRIN and pAKT levels in MCF-7, MMC, MDA-MB-231, and BT-549 cell lines. Bands were quantified using Image Studio™ Lite (LI-COR Biosciences, Lincoln, NE), where relative OD values were obtained. The data were then normalized against β-actin. Data represent the mean ± SD of three independent experiments. The lettering scheme is shown above each table where lower-case letters (e.g., a, b, c, etc.) indicate analysis done by one-way ANOVA followed by Newman-Keuls post hoc t-test. The upper-case letters (e.g., A, B, C) indicate two-tailed t-tests while the symbols (#, *, $) indicate one-tailed t-tests, where significance was defined as $p<0.05$.

pERK1/2	MCF-7	0.0039±0.0031	0.0021±0.0021	0.0018±0.0013	0.0038±0.0025	0.0019±0.0009	0.0014±0.0007
pERK5		0.0054±0.0025	0.0082±0.0027	0.0065±0.0019	0.0055±0.0008	0.004±0.0004	0.0046±0.0003
p-AKT		0.00094±0.0008	0.0030±0.0011	0.0022±0.0012	0.0025±0.0012	0.00063±0.0005 ($)	0.00085±0.0012
NF-κB		0.19±0.11	0.36±0.12	0.29±0.10	0.24±0.09	0.19±0.06	0.22±0.01
RUNX2		0.19±0.04	0.17±0.04	0.19±0.02	0.15±0.02 (*A)	0.12±0.04	0.15±0.04
β1-INTEGRIN		0.13±0.05	0.14±0.10	0.094±0.01	0.072±0.02	0.079±0.03	0.083±0.05
		Veh (*A)	1 nM C4 (#B)	1 nM C4+pictlisib	10 μM C4 ($C)	10 μM C4+pictilisib	pictilisib
pERK1/2	MMC	0.0017±0.0009	0.0010±0.0003	0.0010±0.0003	0.00084±0.001	0.0015±0.001	0.0021±0.001
pERK5		0.0038±0.0021	0.0023±0.0020	0.0032±0.0018	0.0039±0.0022	0.0033±0.0020	0.0038±0.0008
p-AKT		0.00018±0.00045	0.000029±0.000051	0.00060±0.00052	0.00030±0.00032	0.00056±0.00098	0.00054±0.00059
NF-κB		0.36±0.11	0.34±0.043	0.35±0.12	0.37±0.085 (*A)	0.33±0.095	0.39±0.12
RUNX2		0.22±0.039	0.20±0.041	0.21±0.005	0.19±0.03	0.22±0.015	0.23±0.056
β1-INTEGRIN		0.25±0.085	0.23±0.028	0.23±0.048	0.26±0.077 (*)	0.23±0.030	0.24±0.095
		Veh (*A)	1 nM C4 (#B)	1 nM C4+pictlisib	10 μM C4 ($C)	10 μM C4+pictilisib	pictilisib
pERK1/2	MDA-MB-231	0.0024±0.0017	0.0021±0.0018	0.0025±0.0018	0.0023±0.00095	0.0014±0.0011 ($C)	0.0029±0.00076
pERK5		0.00092±0.00076	0.0013±0.00015	0.0020±0.0001	0.0016±0.00019	0.0020±0.00052	0.00092±0.00018
p-AKT		0.000049±0.00012	0.00077±0.0012	0.00030±0.00022	0.00058±0.00056	0.00028±0.00031	0.00018±0.00024
NF-κB		0.093±0.03	0.085±0.026	0.10±0.042	0.089±0.033	0.11±0.030	0.08±0.032
RUNX2		0.16±0.055	0.11±0.002	0.12±0.019	0.17±0.075	0.16±0.029	0.12±0.034
β1-INTEGRIN		0.022±0.009	0.025±0.020	0.036±0.013	0.030±0.019	0.035±0.022	0.015±0.020
		Veh (*A)	1 nM C4 (#B)	1 nM C4+pictlisib	10 μM C4 ($C)	10 μM C4+pictilisib	pictilisib
pERK1/2	BT-549	0.00087±0.0015	0.00018±0.00032	0.0021±0.0003 (#B)	0.0036±0.0052	0.0023±0.0021	0±0
pERK5		0.0051±0.0026	0.0067±0.0025	0.0043±0.0024	0.0050±0.0035	0.0033±0.0018	0.0033±0.0030
p-AKT		0.00089±0.0013	0.0020±0.0016	0.0014±0.0020	0.0013±0.0022	0.00023±0.00041	0.0040±0.0047
NF-κB		0.54±0.25	0.83±0.53	0.50±0.091	0.59±0.43	0.46±0.049	0.75±0.45
RUNX2		0.31±0.10	0.45±0.30	0.27±0.077	0.34±0.21	0.34±0.17	0.50±0.15
β1-INTEGRIN		0.38±0.21	0.58±0.48	0.35±0.11	0.43±0.30	0.36±0.069	0.57±0.34

Table 7: The effect of PI3K (pictilisib) on C5-mediated effects on pERK1/2, pERK5, NF-κB, RUNX2, β1-INTEGRIN and pAKT levels in MCF-7, MMC, MDA-MB-231, and BT-549 cell lines. Bands were quantified using Image Studio™ Lite (LI-COR Biosciences, Lincoln, NE), where relative OD values were obtained. The data were then normalized against β-actin. Data represent the mean ± SD of three independent experiments. The lettering scheme is shown above each table where lower-case letters (e.g., a, b, c, etc.) indicate analysis done by one-way ANOVA followed by Newman-Keuls post hoc t-test. The upper-case letters (e.g., A, B, C) indicate two-tailed t-tests while the symbols (#, *, $) indicate one-tailed t-tests, where significance was defined as $p<0.05$.

pERK1/2	MCF-7	0.0039±0.0031	0.0019±0.0018	0.0031±0.0018	0.0026±0.0013	0.0031±0.0015	0.0014±0.0007
pERK5		0.0054±0.0025	0.0084±0.0049	0.0090±0.0040	0.0090±0.0048	0.0094±0.0050	0.0046±0.0003
p-AKT		0.00094±0.0008	0.0022±0.0018	0.00068±0.0007	0.00040±0.0006	0.0013±0.0006	0.00085±0.0012
NF-κB		0.19±0.11	0.27±0.14	0.38±0.25	0.27±0.16	0.65±0.43	0.22±0.01
RUNX2		0.19±0.04	0.16±0.07	0.18±0.09	0.16±0.05	0.21±0.10	0.15±0.04
β1-INTEGRIN		0.13±0.05	0.070±0.05	0.069±0.03	0.082±0.01	0.22±0.17	0.083±0.05
		Veh (*A)	1 nM C5 (#B)	1 nM C5+pictlisib	10 µM C5 ($C)	10 µM C5+pictilisib	pictilisib (d)
pERK1/2	MMC	0.0017±0.0009	0.0020±0.0004	0.0029±0.0027	0.0022±0.0010	0.0013±0.0006	0.0021±0.0010
pERK5		0.0038±0.0021	0.0042±0.0004	0.0037±0.0026	0.0034±0.0007	0.0039±0.0010	0.0038±0.0008
p-AKT		0.00018±0.00045	0.0012±0.0011	0.0017±0.0022	0.0013±0.0019	0.00071±0.00096	0.00054±0.00059
NF-κB		0.36±0.11	0.46±0.045 (*A)	0.38±0.16	0.34±0.12	0.36±0.072	0.39±0.12
RUNX2		0.22±0.039	0.23±0.02	0.20±0.061	0.22±0.066	0.20±0.034	0.23±0.056
β1-INTEGRIN		0.25±0.085	0.33±0.07 (*)	0.29±0.13	0.22±0.088	0.24±0.043	0.24±0.095
		Veh (*A)	1nM C5 (#B)	1 nM C5+pictlisib	10 µM C5 ($C)	10 µM C5+pictilisib	pictilisib (d)
pERK1/2	MDA-MB-231	0.0024±0.0017	0.0022±0.00038	0.0013±0.0015	0.0021±0.00082	0.0029±0.0015	0.0029±0.00076
pERK5		0.00092±0.00076	0.0020±0.00080	0.0047±0.0021	0.0020±0.0012	0.0022±0.00038	0.00092±0.00018
p-AKT		0.000049±0.00012	0.00037±0.00035	0.00019±0.00033	0.00025±0.00041	0.000073±0.000075	0.00018±0.00024
NF-κB		0.093±0.030	0.19±0.072 (a)	0.27±0.063 (bd)	0.14±0.028	0.16±0.060	0.08±0.032
RUNX2		0.16±0.055	0.19±0.025	0.22±0.042 (#)	0.15±0.069	0.17±0.077	0.12±0.034
β1-INTEGRIN		0.022±0.009	0.037±0.021	0.11±0.011 (#B)	0.061±0.010 (*)	0.073±0.037	0.015±0.020
		Veh (*A)	1 nM C5 (#B)	1 nM C5+pictlisib	10 µM C5 ($C)	10 µM C5+pictilisib	pictilisib (d)
pERK1/2	BT-549	0.00087±0.0015	0.00097±0.0014	0.00099±0.0014	0.00055±0.0009	0.00063±0.0011	0±0
pERK5		0.0051±0.0026	0.0026±0.0017 (*A)	0.0040±0.0049	0.0062±0.0061	0.0057±0.0061	0.0033±0.0030
p-AKT		0.00089±0.0013	0.00027±0.00038	0.0015±0.0026	0.00071±0.0012	0.00063±0.0010	0.0040±0.0047
NF-κB		0.54±0.25	0.51±0.22	0.59±0.65	0.58±0.46	0.57±0.39	0.75±0.45
RUNX2		0.31±0.10	0.24±0.024	0.29±0.25	0.36±0.22	0.38±0.17	0.50±0.15
β1-INTEGRIN		0.38±0.21	0.40±0.18	0.41±0.42	0.43±0.33	0.40±0.30	0.57±0.34